Title	Mass of galaxy lenses in modified gravity: any need for dark mass?
Author(s)	Chiu, MC; Ko, CM; Tian, Y; Zhao, HS
Citation	Physical Review D (Particles, Fields, Gravitation and Cosmology), 2011, v. 83 n. 6, article no. 063523
Issued Date	2011
URL	http://hdl.handle.net/10722/139625
Rights	Creative Commons: Attribution 3.0 Hong Kong License

Mass of galaxy lenses in modified gravity: Any need for dark mass?

Mu-Chen Chiu,[1,2] Chung-Ming Ko,[1,3,4,6,*] Yong Tian,[3,†] and HongSheng Zhao[5,‡]

[1]*Institute of Astronomy, National Central University, Jhongli, Taiwan 320, R.O.C.*
[2]*Scottish University Physics Alliance, Institute for Astronomy, the Royal Observatory, University of Edinburgh, Blackford Hill, Edinburgh,EH9 3HJ, UK*
[3]*Department of Physics, National Central University, Jhongli, Taiwan 320, R.O.C.*
[4]*Center for Complex Systems, National Central University, Jhongli, Taiwan 320, R.O.C.*
[5]*Scottish University Physics Alliance, University of St. Andrews, KY16 9SS,UK*
[6]*Department of Physics, University of Hong Kong, Pokfulam Road, Hong Kong, China*

(Received 26 July 2010; published 25 March 2011)

Using strong lensing data, Milgrom's modified Newtonian dynamics (MOND) and its covariant TeVeS (tensor-vector-scalar theory) are examined here as an alternative to the conventional ΛCDM paradigm. We examine 10 double-image, gravitational lensing systems in which the lens masses have been estimated by stellar population synthesis models. While mild deviations exist, we find no strong case of outliers to the TeVeS theory.

DOI: 10.1103/PhysRevD.83.063523 PACS numbers: 95.35.+d

I. INTRODUCTION

The concordant ΛCDM paradigm [see e.g.,[1]] has been accepted as a successful framework to understand the evolution of the Universe. However, in this standard model there are two unexplained dark sectors, dubbed dark matter and dark energy, which still need a more fundamental understanding. One of the various explanations of these is the approach of modified gravity, including Bekenstein's TeVeS (tensor-vector-scalar theory)[2]. Unlike most theories of modified gravity that are proposed for explaining dark energy, TeVeS was originally proposed to explain dark matter instead. Indeed, TeVeS was built up by Bekenstein as a viable relativistic version of Milgrom's modified Newtonian dynamics (MOND) [3].

In MOND, the demand for the exotic dark matter is replaced by the modification of Newton's second law:

$$\tilde{\mu}(|\mathbf{a}|/\mathfrak{a}_0)\mathbf{a} = -\boldsymbol{\nabla}\Phi_{\mathrm{N}}, \tag{1}$$

with $\mathfrak{a}_0 \approx 1.2 \times 10^{10}\ \mathrm{m\,s^{-2}}$. The function $\tilde{\mu}(x)$, sometimes called the interpolation function, possesses the features that $\tilde{\mu}(x) \approx x$ for $x \ll 1$ (the deep MOND regime), and $\tilde{\mu}(x) \to 1$ when $x \to 1$ (the Newtonian regime). Here, $x = |\mathbf{a}|/\mathfrak{a}_0$, the ratio of the acceleration to $\mathfrak{a}_0$, is a measure of modified gravity. In contrast with the ΛCDM paradigm, MOND and TeVeS, along with many other recent theories that recover MOND in its limit (such as the bimetric theory of [4] and the dark fluid theory of [5]), are called the MONDian paradigm. The ideology of this paradigm is to demolish the requirement of dark matter through modifying theories of gravity.

Observationally, the MONDian paradigm is not only able to explain the cosmic microwave background (CMB) successfully with low-mass neutrinos [6,7], but is also even more successful than the ΛCDM paradigm on the dynamics of spiral galaxies [8,9]. The bullet cluster shows a strong evidence of dark matter by a weak lensing analysis [10]. However, this system might also be understood in the framework of TeVeS by the help from low-mass neutrinos. On cluster scales, low-mass neutrinos can aggregate and their mass could easily exceed the mass of the baryons. Angus *et al.* [11] found 2 eV ordinary neutrinos could create enough weak lensing in MOND in the bullet cluster to be consistent with the observed offset of the peaks of the lensing signal and x-ray signal, as the mass distribution of the dissipationless neutrino does not follow the distribution of the collisional gas. More recently, Angus [12] and Angus *et al.* [13] examined MONDian models with one low-mass sterile neutrino of 11 eV to be the hot dark matter, and nearly zero-mass for ordinary neutrinos, and also found consistency with cluster data and CMB; in fact such a low-mass neutrino model is also consistent with the data on the galaxy cluster substructure lensing [14], and especially with the very constraining straight arc of Abell 2390 [15]. What is common of all these proposals for neutrinos is that these low-mass neutrinos never cluster enough on galaxy scales because of their low phase space density [15], which scales with the neutrino mass to the power four, as first noted by Tremaine and Gunn [16]. The nonclustering of low-mass neutrinos on galaxy scales is the most robust distinction of MOND vs cold dark matter in galaxies. In this regard, it seems very important to check the conclusion of Ferreras *et al.* [17] that cold dark matter is still needed in elliptical galaxies for strong lensing, especially, when earlier works of Zhao *et al.* [18] and Shan *et al.* [19] found much weaker evidence for cold dark matter from strong lensing.

The earliest works on gravitational lensing in MOND were studied by Qin *et al.* [20] and Mortlock and Turner

*cmko@astro.ncu.edu.tw
†yonngtian@gmail.com
‡hz4@st-andrews.ac.uk

[21]. Although their work was performed even before the appearance of a viable, general covariant MOND, and their calculations on the angle of deflection were artificially forced into the deep MOND regime when the acceleration was less than $\mathfrak{a}_0$, i.e., $\tilde{\mu}(x) = x$ for $x \leq 1$ (not $x \ll 1$), Qin *et al.* [20] and Mortlock and Turner [21] could produce a good guess on how to calculate lensing in MOND. After the advent of TeVeS, the first calculation on light bending in TeVeS was done by Bekenstein himself, followed up by Chiu *et al.* [22]. Based on a point mass model, Chiu *et al.* [22] applied the formalism of gravitational lensing in TeVeS to the theoretical discussion on angle of deflection and magnification, as well as time delay.

On the other hand, taking a more phenomenological approach, Zhao *et al.* [18] showed that TeVeS is consistent with a sample of double-image lenses in the CASTLES catalog by modeling lenses with the Hernquist model. Feix *et al.* [23] studied the effects of asymmetric systems on gravitational lensing. Shan *et al.* [19] then applied nonspherical models to investigate strong lensing in TeVeS and found 10 out of 15 systems to be consistent with it. All of the other 5 systems are found to reside in or close to clusters of galaxy, where external fields could have significant influence. Furthermore, the effect of large filaments on gravitational lensing was studied by Feix *et al.* [24]. They argued that filamentary structures might have complex but significant contributions to the system such as the bullet cluster, so the need for dark matter in the bullet cluster might be spared again in MOND. However, all of the above work is in a nonrelativistic approximation of TeVeS. In a conference paper, Chiu *et al.* [25] also showed that the lens data from CASTLES and SLACS catalogs are consistent with TeVeS, but they did not provide the details.

The first effort to calculate gravitational lensing from first principles was given by Mavromatos *et al.* [26]. Along with other works in this series [17,27], it has been shown that TeVeS might still need dark matter to explain the lensing systems from CASTLES, and there is a lack of consistent results between dynamical and gravitational lensing analysis.

Because of the importance of studying gravitational lensing in TeVeS, and the inconsistency of the results in this field, in this paper we use the relativistic approach developed by Bekenstein [2] and Chiu *et al.* [22] and, applying the Hernquist mass distribution as the lens model (used for TeVeS firstly by Zhao *et al.* [18]), study the 10 double-image systems from a total of 18 objects studied in Ferreras *et al.* [28].

The structure of the paper is organized as below. In Sec. II, we briefly outline the basic assumptions and formalism of gravitational lensing in TeVeS. We also discuss how gravitational lensing in TeVeS depends on different choices of $\tilde{\mu}(|\mathbf{a}|/\mathfrak{a}_0)$ and its application to double-image systems. We then give our result in Sec. III and subsequent discussion in Sec. IV.

II. FORMALISM OF GRAVITATIONAL LENSING IN TEVES

A. Basic assumpsions

The analysis in this paper uses the following assumptions: (1.) Elliptical galaxies contain very little gas, so their baryonic budget is only through the total stellar mass. When taking neutrino mass into consideration, there is also very little mass in the form of ordinary neutrinos (about 10^8 solar mass maximum). Thus, the lensing power of ellipticals in MOND is essentially determined by the stellar mass. (2.) Since there is little cold dark matter in MOND, we should use a MONDian cosmology to calculate angular distance in lensing analysis. For this purpose, we use a viable MONDian cosmology proposed by Skordis *et al.* [7], dubbed νHDM. In this cosmological model, 2 eV neutrinos are included and the background evolution of the Universe can be fitted well by $\{h, \Omega_b, \Omega_\nu, \Omega_\Lambda\} = \{0.7, 0.05, 0.17, 0.78\}$, which is independent of the choice of the interpolation function $\tilde{\mu}(x)$ (see Eq. (1)). (3.) Finally, we also assume a simple spherically symmetric mass distribution. Because of assumptions (1.) and (3.), we adopt the Hernquist model as the lens model.

B. Lensing in TeVeS

As suggested by its name, TeVeS is a gravity theory dynamically incorporating scalar, vector, and tensor fields. TeVeS is also a bimetric covariance theory where the Einstein metric $g_{\alpha\beta}$ is related to the physical metric $\tilde{g}_{\alpha\beta}$ by a nonconformal transformation,

$$\tilde{g}_{\alpha\beta} = e^{-2\phi}(g_{\alpha\beta} + \mathcal{U}_\alpha \mathcal{U}_\beta) - e^{2\phi}\mathcal{U}_\alpha \mathcal{U}_\beta, \tag{2}$$

with a normalization condition on the vector field,

$$g^{\alpha\beta}\mathcal{U}_\alpha \mathcal{U}_\beta = -1. \tag{3}$$

Although gravitational fields, including the scalar field ϕ and vector field $\mathcal{U}_\alpha$, are governed explicitly by the Einstein metric, the dynamical behavior of matter is explicitly controlled by the physical metric. In other words all kinds of matter, be it photon, proton, or neutrino, are minimally coupled to the physical metric rather than the Einstein metric. While considering strong lensing in TeVeS, we take the assumption that, in the weak field limit, the physical metric of a static, spherically symmetric system can be expressed in the isotropic form ($c = 1$):

$$\tilde{g}_{\alpha\beta}dx^\alpha dx^\beta = -(1 + 2\Phi)dt^2 + (1 - 2\Phi) \times [d\varrho^2 + \varrho^2(d\theta^2 + \sin^2\theta d\varphi^2)], \tag{4}$$

where $\Phi(\varrho) = \Xi\Phi_N + \phi$ and $\Xi \equiv e^{-2\phi_c}(1 + K/2)^{-1}$ with ϕ_c as the asymptotic boundary value of ϕ, and $K < 10^{-3}$ from the constraint of the parametrized post-Newtonian parameters [2]. It has been shown that the cosmological value of the scalar field, ϕ_c, is tightly linked to the vector field coupling constant K, preventing ϕ_c

evolving as predicted by the equation of motion of scalar field [29]. This and other possible dynamic problems in the original TeVeS can be solved by a more generalized version: TeVeS with Æther-type vector action, where four vector coupling constants rather than just one are involved [29–31]. However, we do not consider this generalized TeVeS here because, in practical, the impact of either K or other additional vector coupling constants on lensing system is less than 1%, which is much smaller than the available precision in this paper. That is, our analysis is insensitive to the difference between the original and generalized TeVeS.

Since, in TeVeS, all species of matter are coupled to the physical metric rather than to Einstein's metric, the connection in the geodesic equation,

$$\frac{d^2x^\mu}{dp^2} + \Gamma^\mu_{\nu\lambda}\frac{dx^\nu}{dp}\frac{dx^\lambda}{dp} = 0, \tag{5}$$

has to be constructed from the physical metric. Here, p is some proper affine parameter. In the case of light deflection by a static, spherically symmetric lens, we can apply Eq. (4) to the geodesic equation, Eq. (5).

Consider a photon which propagates on a null geodesic, and moves in the equatorial plane, i.e., $\theta = \pi/2$. The geodesic equation or equations of motion can be written as

$$(1 + 2\Phi)\dot{t} = E, \tag{6}$$

$$(1 - 2\Phi)\varrho^2\dot{\varphi} = L, \tag{7}$$

$$(1 - 2\Phi)\dot{\varrho}^2 + (1 + 2\Phi)\varrho^{-2}L^2 - (1 - 2\Phi)E^2 = 0, \tag{8}$$

where the overdot denotes the derivative with respect to p. Recall the fact that at the closest approach $\dot{\varrho} = 0$, $\varrho = \varrho_0$, we can express the ratio of the angular momentum L to energy E as

$$b^2 \equiv \frac{L^2}{E^2} = \frac{\varrho_0^2(1 - 2\Phi_0)}{(1 + 2\Phi_0)}, \tag{9}$$

where $\Phi_0 \equiv \Phi(\varrho_0)$. Here, b is called the impact parameter. Combining Eqs. (7)–(9) gives the orbit of the photon,

$$-(1 - 4\Phi) + (1 - 4\Phi_0)\left(\frac{\varrho_0}{\varrho}\right)^2\left[\frac{1}{\varrho^2}\left(\frac{d\varrho}{d\varphi}\right)^2 + 1\right] = 0, \tag{10}$$

for which the solution in quadrature is

$$\varphi = \int^\varrho \left\{\left(\frac{\varrho}{\varrho_0}\right)^2[1 - 4(\Phi - \Phi_0)] - 1\right\}^{-1/2}\frac{d\varrho}{\varrho}. \tag{11}$$

If we take the Taylor expansion of Eq. (11) to the first order in Φ, we get the angle spanned by the orbit of the photon

$$\delta\varphi \simeq \int_{\varrho_0}^\varrho \frac{2\varrho_0 d\varrho}{\varrho(\varrho^2 - \varrho_0^2)^{1/2}} + \varrho_0\int_{\varrho_0}^\varrho \frac{4\varrho(\Phi - \Phi_0)}{(\varrho^2 - \varrho_0^2)^{3/2}}d\varrho. \tag{12}$$

The first term is the orbit without gravity, i.e., a straight line ($\varphi \to \pi$ as $\varrho \to \infty$). The second term is the angle of the deviation due to the gravity. Hence, to first order in Φ, the deflection angle is

$$\begin{aligned}\Delta\varphi \equiv \delta\varphi - \pi &= \varrho_0\int_{\varrho_0}^\varrho \frac{4\varrho(\Phi - \Phi_0)}{(\varrho^2 - \varrho_0^2)^{3/2}}d\varrho \\ &= \varrho_0\int_{\varrho_0}^\varrho \frac{4|\nabla\Phi|}{(\varrho^2 - \varrho_0^2)^{1/2}}d\varrho - \frac{4\varrho_0\Phi}{(\varrho^2 - \varrho_0^2)^{1/2}},\end{aligned} \tag{13}$$

where we have made use of integration by parts. Since for very large ϱ, Φ behaves as $\ln\varrho$ (as can be seen from Eq. (1)), it is legitimate to ignore the second term of Eq. (13) for strong lensing systems [22]. We then have the kernel equation of strong gravitational lensing in TeVeS (up to first order in $\nabla\Phi$),

$$\Delta\varphi = 4\varrho_0\int_{\varrho_0}^\infty \frac{|\nabla\Phi|}{(\varrho^2 - \varrho_0^2)^{1/2}}d\varrho. \tag{14}$$

Recall that ϱ_0 is the distance of the closest approach, and $\nabla\Phi$ is the MONDian gravity.

C. Gravity in TeVeS

In last subsection we showed that, under the assumption of the validity of Eq. (4), the difference between the angle of deflection in general relativity (GR) and that in TeVeS only arises from $\nabla\Phi$. In this subsection, we are going to discuss the relationship between Newtonian gravity, $\nabla\Phi_N$, and MONDian gravity, $\nabla\Phi$, and its application to strong lensing.

It has been shown that in the quasistatic limit the MONDian potential in TeVeS can be expressed as a combination of the Newtonian potential and a scalar field [2],

$$\Phi = \Xi\Phi_N + \phi, \tag{15}$$

where Ξ is a parameter in TeVeS that is approximately 1 and ϕ is a scalar field. Moreover, the scalar field itself is linked to the Newtonian potential via a free function μ [2],

$$\nabla\phi = (k/4\pi\mu)\nabla\Phi_N, \tag{16}$$

where μ is a function of $|\nabla\phi|$. This free function μ should be chosen carefully in order to reproduce Newtonian and MONDian behavior in the approximation to quasistatic limits. In fact, Eqs.. (15), (16), and (1) give the relation between μ and $\tilde{\mu}$ of the modified Poisson equation or Milgrom's law Eq. (1)

$$\frac{1}{\tilde{\mu}} = \Xi + \frac{k}{4\pi\mu}. \tag{17}$$

TeVeS has only two parameters (k and Ξ) and one free function (μ). Therefore, the MONDian behavior controlled by $\tilde{\mu}$ in Milgrom's law Eq. (1) could be achieved via choosing suitable parameters and free function in TeVeS. On the other hand, we are able to express the modified gravity $\nabla\Phi$ (even in TeVeS) as a function of Newtonian gravity $\nabla\Phi_N$ via $\tilde{\mu}$. In the following, we discuss the three commonly used interpolation functions, $\tilde{\mu}$.

In Bekenstein's TeVeS paper [2], he proposed the following interpolation function

$$\tilde{\mu}(x) = \frac{-1 + \sqrt{1 + 4x}}{1 + \sqrt{1 + 4x}}, \tag{18}$$

where $x \equiv |\mathbf{a}|/\mathfrak{a}_0$. With Bekenstein's form, we can write the MONDian gravity as a function of Newtonian gravity,

$$-\mathbf{a} = \boldsymbol{\nabla}\Phi = \boldsymbol{\nabla}\Phi_N(1 + \sqrt{\mathfrak{a}_0/|\boldsymbol{\nabla}\Phi_N|}), \tag{19}$$

by combining Eqs. (15)–(18). Although Bekenstein's form yields a simple relation between $\boldsymbol{\nabla}\Phi$, and $\boldsymbol{\nabla}\Phi_N$, it fails to fit the rotation curves of spiral galaxies [9,32]. Thus, in order to apply the MONDian lens equations to observational data, we must also study the simple form and the standard form, which fit the rotation curves better. Again, by putting the simple form [32],

$$\tilde{\mu}(x) = \frac{x}{1 + x}, \tag{20}$$

into Eqs. (15)–(17), we obtain

$$-\mathbf{a} = \boldsymbol{\nabla}\Phi = \frac{\boldsymbol{\nabla}\Phi_N}{2}(1 + \sqrt{1 + 4\mathfrak{a}_0/|\boldsymbol{\nabla}\Phi_N|}). \tag{21}$$

Similarly, the standard form [3],

$$\tilde{\mu}(x) = \frac{x}{\sqrt{1 + x^2}}, \tag{22}$$

leads to $(\boldsymbol{\nabla}\Phi)^2/\mathfrak{a}_0 = \sqrt{1 + (\boldsymbol{\nabla}\Phi/\mathfrak{a}_0)^2}\boldsymbol{\nabla}\Phi_N$, which tells us that for each $\boldsymbol{\nabla}\Phi_N$, there are two corresponding values of $\boldsymbol{\nabla}\Phi$. This bivalue problem simply reflects the finding of Zhao and Famaey [33] that the standard form is problematic for TeVeS because it leads to $\mu(\nabla\phi/\mathfrak{a}_0)$ becoming a nonunique function of $\tilde{\mu}(\nabla\Phi/\mathfrak{a}_0)$. Nevertheless, we still include the standard form as a point of reference and do the comparisons with the other two $\tilde{\mu}$ functions by treating it as an empirical function. Moreover, since one of the two solutions contains only imaginary numbers, we can always choose the other one as physical solution obtaining, in the standard form,

$$-\mathbf{a} = \boldsymbol{\nabla}\Phi = \frac{\boldsymbol{\nabla}\Phi_N}{\sqrt{2}}\sqrt{1 + \sqrt{1 + 4(\mathfrak{a}_0/|\boldsymbol{\nabla}\Phi_N|)^2}}. \tag{23}$$

All of these three forms can be included in the following two-parameter form:

$$\tilde{\mu}(x) = \left[1 - \frac{2}{(1 + \eta x^\alpha) + \sqrt{(1 - \eta x^\alpha)^2 + 4x^\alpha}}\right]^{1/\alpha}. \tag{24}$$

Here, $(\alpha, \eta) = (1, 0), (1, 1), (2, 1)$ and $(\infty, 1)$ correspond to the Bekenstein form, simple form, standard form and the naive sharp-break form $\tilde{\mu} = \min(1, x)$, respectively. Recall that we have set $c = 1$. We note that Zhao and Famaey[33] have proposed a similar expression in which they combined the Bekenstein form and simple form. We may call Eq. (24) the *invertible canonical interpolation function* which goes from the naive sharp-break to the smooth Bekenstein form. The corresponding μ can be found by Eq. (17). Figure 1 shows some examples of the *invertible canonical interpolation function*. The nicest feature of our invertible canonical interpolation function is that it has a very simple counterpart in the recent quasi-MOND theory or its relativistic version, bimetric MOND [4,34]. Inverting Eq. (1) with $\tilde{\mu}$ given by Eq. (24) gives

$$-\mathbf{a} = \boldsymbol{\nabla}\Phi = \nu\boldsymbol{\nabla}\Phi_N, \tag{25}$$

where

$$\nu(x_N) \equiv \left[1 - \frac{\eta}{2} + \sqrt{x_N^{-\alpha} + \left(\frac{\eta}{2}\right)^2}\right]^{1/\alpha}, \tag{26}$$

and $x_N \equiv |\boldsymbol{\nabla}\Phi_N|/\mathfrak{a}_0$. This analytical result can greatly simplify the calculations in MOND.

Note that some earlier [20,21] and recent [17] physics literature formulated Milgrom's law as

$$\boldsymbol{\nabla}\Phi = \tilde{\mu}^{-1/2}(x_N)\boldsymbol{\nabla}\Phi_N. \tag{27}$$

However, this formulation is valid *only* for the sharp-break function $\tilde{\mu} = \min(1, \boldsymbol{\nabla}\Phi/\mathfrak{a}_0)$, for which $\boldsymbol{\nabla}\Phi = \max(\boldsymbol{\nabla}\Phi_N, \sqrt{\mathfrak{a}_0\boldsymbol{\nabla}\Phi_N})$. In this particular situation,

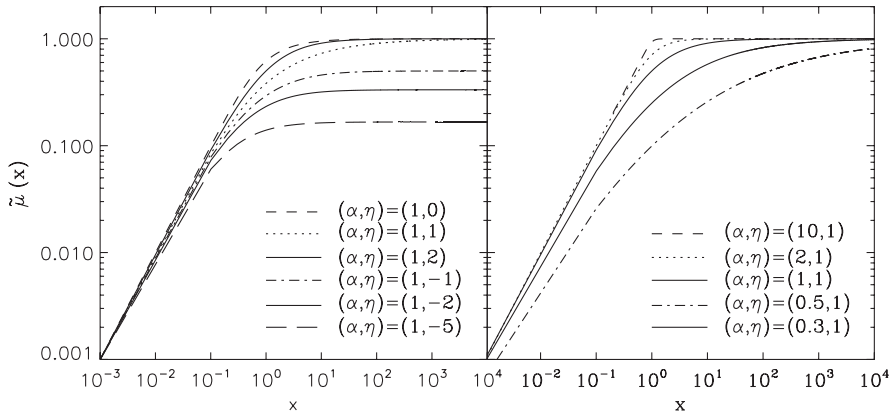

FIG. 1. The strength of the MONDian gravity in different forms of $\tilde{\mu}(x)$.

$$\tilde{\mu}^{-1}(\nabla\Phi/\mathfrak{a}_0) = \mathfrak{a}_0/\nabla\Phi = \sqrt{\mathfrak{a}_0\nabla\Phi_N} = \tilde{\mu}^{-1/2}(\nabla\Phi_N/\mathfrak{a}_0), \quad (28)$$

which does not hold for general choices of $\tilde{\mu}(x)$.

In Fig. 2, we compare the MONDian gravity, $|\nabla\Phi|$, of the three different forms. We also plot the results of the standard form and simple form of the formalism adopted in Ferreras *et al.* [17], that is Eq. (27). For the same form and mass, the MONDian gravity is always stronger than that of Ferreras *et al.* [17].

D. Cosmology in TeVeS

In TeVeS, the scalar and vector fields are assumed to partake of the symmetry of the spacetime. Therefore, it is still legitimate to apply the Friedmann-Robertson-Walker metric in the Einstein frame to the t-t component of the modified Einstein equations to produce the modified Friedmann equation delineated by $g_{\alpha\beta}$:

$$\frac{\dot{a}^2}{a^2} = \frac{8\pi G}{3}\rho_m e^{-2\phi} + \frac{8\pi G}{3}\rho_\phi + \frac{\Lambda}{3} - \frac{K}{a^2}, \quad (29)$$

where ρ_ϕ is scalar field energy density, and ρ_m is matter density, including the baryonic density, ρ_b, and the density of 2 eV neutrinos, ρ_ν. Here, the overdot denotes d/dt and a is the scale factor. Since the vector field is considered to be parallel with the cosmological time, according to Eq. (2) the physical Friedmann-Robertson-Walker metric is related to its counterpart in the Einstein frame by simply replacing

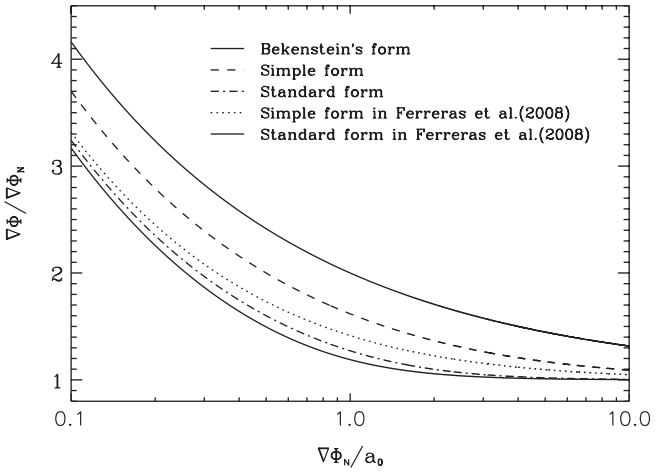

FIG. 2. The invertible canonical interpolation function for various values of (α, η). Here, $x \equiv \nabla\Phi/\mathfrak{a}_0$. $(\alpha, \eta) = (1, 0)$, $(1, 1)$ and $(2, 1)$ correspond, respectively, to Bekenstein's form (dashed line in the left panel), the simple form (solid lines in the both panels), and the standard form (dotted line in the right panel); $(\alpha, \eta) = (10, 1)$ (dashed line in the right panel) shows a profile that is quite near to the naive sharp-break form $\tilde{\mu} = \min(1, x)$. The left panel also shows that a negative value of η would fail to lead to the Newtonian limit (that is, $\tilde{\mu} \to 1$ as $x \gg 1$).

$$d\tilde{t} = e^{\phi}dt; \qquad \tilde{a} = e^{-\phi}a, \quad (30)$$

so the Hubble rates in two frames are related by

$$\frac{\dot{\tilde{a}}}{\tilde{a}} = e^{-\phi}\left(\frac{\dot{a}}{a} - \dot{\phi}\right). \quad (31)$$

Skordis *et al.* [7] have shown that in order to avoid a significant effect of the integrated Sachs Wolfe term on the CMB power spectrum, ρ_ϕ must be extremely small compared with the matter density with ϕ evolving slowly with time. According to Eq. (31), therefore, the Hubble rates in physical and Einstein's frames are nearly identical. Furthermore, although we do not know exactly how ρ_ϕ evolves over time, we can neglect this term because its exact value would be overwhelmed by the uncertainty of ρ_m and Λ for a non-cold dark matter (CDM) universe [7,35,36]. Since in TeVeS, the μ function is determined by the scalar field, ϕ, the negligibility of ρ_ϕ also means that the Hubble expansion is independent of the choice of μ. Moreover, because massive neutrinos stopped free-streaming and became nonrelativistic around $z \sim 100$ [37], which is much earlier than the lensing systems we study here, the density of 2 eV neutrinos should scale with a^{-3}. Remembering that baryonic matter density also scales with a^{-3}, and that there is strong evidence to support the Universe being flat ($K = 0$) [38,39], we can then express the Hubble rate as

$$\tilde{H}^2 \simeq H^2 \simeq H_0^2[(\Omega_\nu + \Omega_m)(1+z)^3 + \Omega_\Lambda]. \quad (32)$$

Accordingly, the angular distance at any redshift can be calculated by

$$D_A \simeq \frac{(1+z)^{-1}}{H_0}\int_0^z dz[(\Omega_\nu + \Omega_m)(1+z)^3 + \Omega_\Lambda]^{-1/2}, \quad (33)$$

which is used for estimating the distance of lenses. In Fig. 3, we compare the angular distance of the νHDM cosmology and that of the standard ΛCDM cosmology.

E. Double-Image systems

In realistic strong lensing systems, most lenses are early type giant elliptical galaxies with very little gas, whose luminosity follows the de Vaucouleurs' law [40], for which the Hernquist model,

$$M(r) = M_0 r^2/(r + r_h)^2, \quad (34)$$

is known to provide a good fit [41]. Here, M_0 is the total mass, and r_h is the Hernquist scale radius, which has a simple relation with the effective radius of surface brightness, $r_h = 0.551 r_e$. According to this model, the Newtonian gravity is given by $|\nabla\Phi_N| = GM_0/(\varrho + r_h)^2$. Since MOND is supposed to have little dark matter, we follow the tradition and adopt the Hernquist model for our lenses (all of which are giant ellipticals).

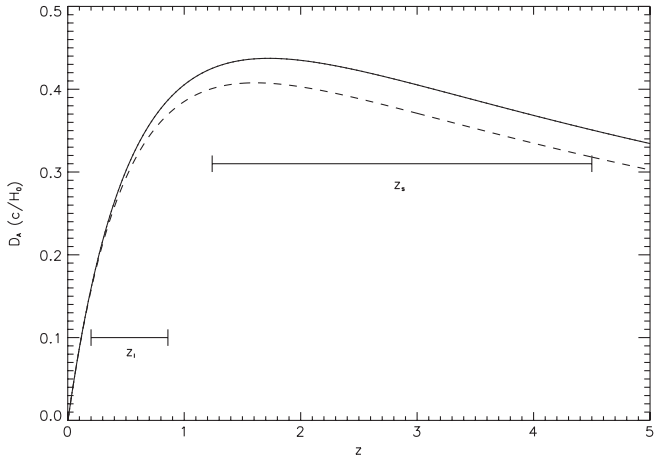

FIG. 3. Angular distances in νHDM ($\Omega_b = 0.05$, $\Omega_\nu = 0.17$, $\Omega_\Lambda = 0.78$, $h = 0.7$, solid line) and the standard cosmology ($\Omega_m = 0.3$, $\Omega_\Lambda = 0.7$, $h = 0.7$, dashed line). Two horizontal bars show the distribution of redshifts of 10 lenses and sources we study in this paper (z_s and z_l are source and lens redshift ranges).

As shown in Sec. II C, the recovered solution $\boldsymbol{\nabla}\Phi$ of Eq. (1) depends on the choice of $\tilde{\mu}$. In general, we can say $|\boldsymbol{\nabla}\Phi| = g(\boldsymbol{\nabla}\Phi_N)$, which can be given specifically by Eqs. (19), (21), and (23), or Eq. (25); and in the case of Einstein's gravity, we simply have $g(\boldsymbol{\nabla}\Phi_N) = \boldsymbol{\nabla}\Phi_N$. Then the deflection angle produced by a spherical lens (Eq. (14)) can be written as

$$\Delta\varphi = \frac{4GM_0}{\varrho_0} f, \tag{35}$$

where

$$f \equiv \int_{\varrho_0}^{\infty} \frac{g(\boldsymbol{\nabla}\Phi_N)\varrho_0^2}{GM_0(\varrho^2 - \varrho_0^2)^{1/2}} d\varrho. \tag{36}$$

Although the angle of deflection, $\Delta\varphi$, is mainly governed by the mass enclosed within ϱ_0, $M(r < \varrho_0)$, we are able to infer the total mass of the lens (M_0) from the Hernquist model if the effective radius of the lens is observed.

In practice, since what we can measure in the sky is not deflection angles but positions of the projected images, it is useful to define $\theta = \varrho_0/D_L$ and $\theta_E = \sqrt{4GM_0D_{LS}/D_LD_S}$, where D_L, D_S, and D_{LS} are distances from observer to lens, observer to source, and lens to source, respectively. Here, θ_E is called the Einstein radius; D_L, D_S, and D_{LS} are calculated from Eq. (33). For a spherical strong lens, two images are located on both sides of the lens (θ_+ and θ_-). The corresponding lens equations are [cf., [22]]

$$\beta = \theta_+ - \frac{D_{LS}}{D_S}\Delta\varphi(\theta_+) = \theta_+ - \frac{\theta_E^2}{\theta_+} f_+, \tag{37}$$

$$\beta = \frac{D_{LS}}{D_S}\Delta\varphi(\theta_-) - \theta_- = \frac{\theta_E^2}{\theta_-} f_- - \theta_-, \tag{38}$$

where β is the source position, and $f_\pm$ can be obtained from Eq. (36) with given $\varrho_{0\pm}$ (or equivalently, $\theta_\pm$). These two lens equations can be combined into

$$\theta_E^2 = \frac{\theta_+\theta_-(\theta_+ + \theta_-)}{(\theta_+ f_- + \theta_- f_+)}. \tag{39}$$

Therefore, with the observed positions of the two images, θ_+, θ_-, and the values of D_L, D_S, D_{LS}, we are able to infer the total mass of the lens, M_0, by computing θ_E. We solve Eq. (39) for the total lens mass by iterative method.

With M_0, in hand, we can then use the Hernquist mass distribution to calculate the lens mass within some particular radius. For example, given a truncated radius $r_{\rm lens}$ in [28], we are able to derive the lensing aperture mass enclosed within this truncated radius by $M_{\rm aperture} = M_0 r_{\rm lens}^2/(r_{\rm lens} + r_h)^2$, and compare it with the initial mass functions (IMFs) aperture mass listed in [28]. Another example is to estimate the gravity contributed by the mass enclosed within the radius of the closest approach, ϱ_{0+} or ϱ_{0-}, that is, $M(\varrho_{0\pm}) = M_0\varrho_{0\pm}^2/(\varrho_{0\pm} + r_h)^2$. Since the main contributor to the angle of deflection is the mass enclosed within the radius of the closest approach, we might define the characteristic radius of the lens in MOND as

$$r_{0+} \equiv \sqrt{\frac{GM_0\varrho_{0+}^2}{\mathfrak{a}_0(\varrho_{0+} + r_h)^2}}; \quad r_{0-} \equiv \sqrt{\frac{GM_0\varrho_{0-}^2}{\mathfrak{a}_0(\varrho_{0-} + r_h)^2}}. \tag{40}$$

There are two characteristic radii because in general $\varrho_{0+} \neq \varrho_{0-}$, so the light rays of the two images might penetrate different regimes. According to this definition, the geometric average of the Newtonian gravity at two radii of the closest approach can be written down concisely in terms of $\theta_{0+} \equiv r_{0+}/D_L$, $\theta_{0-} \equiv r_{0-}/D_L$, and $\theta_\pm$:

$$\langle\boldsymbol{\nabla}\Phi_N\rangle/\mathfrak{a}_0 \equiv \sqrt{\boldsymbol{\nabla}\Phi_{N+}\boldsymbol{\nabla}\Phi_{N-}}/\mathfrak{a}_0 = \frac{\theta_{0+}\theta_{0-}}{\theta_+\theta_-}, \tag{41}$$

which could approximately tell us in which regime the double-image lensing systems are located. Roughly speaking, if $\langle\boldsymbol{\nabla}\Phi_N\rangle \ll \mathfrak{a}_0$, then the system belongs to the deep MOND regime; on the other hand, if $\langle\boldsymbol{\nabla}\Phi_N\rangle \gg \mathfrak{a}_0$, then it is within the Newtonian regime.

III. DATA AND RESULTS

We apply our formalism to 10 double-image lenses from the CASTLES catalog [42], for which not only the images of the lenses are resolved (from which the effective radius of the lens can be found by fitting the light profile [42]), but also the stellar masses are estimated by stellar population synthesis models with different IMFs [28]. We pick only these 10 systems out of the CASTLES catalog because we want to compare our lensing masses with stellar masses from [28], and our assumption of a spherically symmetric lens model is only valid for double-image lensing systems.

Table I shows the details of these 10 systems. In column 2, we cite the effective radius from [42], and in columns 3 and 4 we list the separation between two deflected images and their shared lens from the CASTLES catalog [43]. We also cite in column 5 the truncated radii from [28] for calculating aperture mass. For a consistent analysis, lensing in TeVeS should be studied in the MONDian cosmology. We adopt a viable MONDian cosmology νHDM as our background cosmology, where the Hubble parameter is described by $\{\Omega_m, \Omega_\nu, \Omega_\Lambda, h\} = \{0.05, 0.17, 0.78, 0.7\}$ through Eq. (7). The distances of the lenses and background galaxies, and distances between them in νHDM are calculated by Eq. (34) and listed in columns 8–10. In order to compare our analysis with previous works such as [17], we also analyze the systems in the standard cosmology ($\Omega_m = 0.3$, $\Omega_\Lambda = 0.7$, $h = 0.7$). The angular distances required for lensing analysis in the standard cosmology are shown in columns 11–13. It also appears that, for the same redshift, the distance in νHDM is always a little bit larger than that in the standard cosmology (see Fig. 3).

We have analyzed the masses of 10 lenses embedded in the νHDM cosmology for three particular forms of $\tilde{\mu}(x)$. Column 2 shows all lenses are well into the MOND regime. In columns 3–5 of Table II, we list the aperture mass and total mass (in parentheses) of the lenses. The definitions of total mass and aperture mass are given in Sec. II E. According to our analysis, the lensing mass estimated from Bekenstein's form is the smallest, followed by the mass from the simple form, and then from the standard form. In column 6, we also list the lensing mass calculated by Einstein's gravity theory based on the same cosmological background. The comparison of M_L estimated from GR and TeVeS supports the idea that the mass discrepancy between the Newtonian and the MONDian paradigm is quite significant ($\approx 12\%$ for the standard form, $\approx 25\%$ for the simple form, and $\approx 40\%$ Bekenstein's form). The error in the effective radius is the main cause of the uncertainty of the estimates of lensing mass here, which is about 10%. Besides which, the precision of the image positions also introduces another much smaller error of around 1%. Moreover, the approximation of a spherical lens could introduce systematic errors that are harder to quantify. However, we are aware of 7 out of 10 double-imaged systems are consistent with systems rounder than 0.7 in the axis ratio of the isophotes of the light distribution [19]. For the other three, we cannot find the information of axis ratios in literature, but this does not mean they must be nonspherical. Furthermore, all the lens galaxies are always very close to the line connecting the two images, implying no strong need to invoke nonspherical lenses. If any of these systems happens to be nonspherical, a comparison between nonspherical [19] and Hernquist lens in [18] can indicate a range of uncertainty of lensing mass between 0–30%.

Ferreras *et al.* [28] estimated the aperture stellar mass by two IMFs: Chabrier [44] and Salpeter [45], and the results are listed in columns 7 and 8 of Table II, respectively. For comparison, we use the total lens mass and Hernquist model to compute the mass enclosed within the truncated radius given in Ferreras *et al.* [28]. We cite the truncated radii in column 5 of Table I. Our estimates of lensing mass are listed in columns 3 to 6 of Table II. When comparing with the stellar mass ($M_{\rm Salp}$) from Salpeter's IMF, we find that, except for Q0142 − 100 and BRI0952 − 0115 (where lensing gives smaller mass), all masses derived from Bekenstein's form are within the uncertainty of $M_{\rm Salp}$. For the simple form, there are 7 systems where masses of lenses overlap with Salpeter's stellar mass; for the standard form, there are 5. On the other hand, when compared with stellar mass ($M_{\rm Chab}$) inferred from Chabrier IMF, Bekenstein's form and the simple form both have 6 systems that yield compatible lensing mass, and the standard form has 5.

TABLE I. Double-image lensing systems in the CASTLES catalog. The effective radii, positions, and redshifts of images are cited from [42,43]; the truncated radii are cited from [28]. The angular distances are calculated in the standard ΛCDM cosmology as well as in νHDM cosmology. We refer the readers to the original paper of [42] for the uncertainty of the effective radius.

							νHDM			ΛCDM		
Lens	θ_e ($''$)	θ_+ ($''$)	θ_- ($''$)	$\theta_{\rm lens}$ ($''$)	z_s	z_l	D_S (c/H_0)	D_L (c/H_0)	D_{LS} (c/H_0)	D_S (c/H_0)	D_L (c/H_0)	D_{LS} (c/H_0)
Q0142 − 100	0.51	1.86	0.38	0.93	2.72	0.49	0.415	0.298	0.367	0.381	0.290	0.265
HS0818 + 1227	0.89	2.22	0.62	1.97	3.12	0.39	0.401	0.259	0.391	0.366	0.254	0.281
FBQ0951 + 2635	0.17	0.89	0.23	0.5	1.24	0.20	0.425	0.159	0.376	0.401	0.157	0.316
BRI0952 − 0115	0.10	0.64	0.36	0.5	4.50	0.38	0.351	0.255	0.374	0.318	0.250	0.255
Q1017 − 207	0.30	0.66	0.19	0.3	2.55	0.86	0.421	0.387	0.279	0.387	0.370	0.193
HE1104 − 1805	0.63	1.09	2.11	2.34	2.32	0.73	0.428	0.363	0.298	0.394	0.349	0.212
LBQ1009 − 025	0.18	1.22	0.32	0.53	2.74	0.78	0.415	0.373	0.303	0.347	0.325	0.192
B1030 + 071	0.45	1.44	0.19	0.81	1.54	0.60	0.436	0.332	0.266	0.408	0.321	0.205
SBS1520 + 530	0.35	1.21	0.39	1.04	1.86	0.72	0.437	0.361	0.266	0.406	0.347	0.197
HE2149 − 274	0.50	1.35	0.34	0.71	2.03	0.50	0.434	0.302	0.342	0.402	0.293	0.257

TABLE II. Lensing mass estimates for three particular forms of $\tilde{\mu}(x)$ in νHDM cosmology. The aperture mass and total mass (in parentheses) of the lens in unit of $10^{10}M_{\odot}$ are listed in columns 3–5. Because of the uncertainty of effective radii, the uncertainty of masses are as much as 10%. For comparison, the last two columns list the stellar mass M_* estimated from two IMF models in [28].

	M_L(TeVeS)/$10^{10}M_{\odot}$				M_L (GR)	M_* [28]	
Lens	$\frac{\langle\nabla\Phi_N\rangle}{\mathfrak{a}_0}$	Bekenstein	Simple	Standard		Chabrier	Salpeter
Q0142 − 100	6.9	11.3 (19.19)	14.2 (24.16)	16.6 (28.29)	19.1 (32.45)	$20.9^{30.8}_{13.0}$	$18.3^{32.2}_{13.2}$
HS0818 + 1227	6.8	18.8 (29.38)	24.0 (37.45)	28.6 (44.65)	32.7 (51.05)	$16.2^{21.2}_{12.6}$	$20.8^{28.1}_{13.4}$
FBQ0951 + 2635	11.2	1.56 (2.19)	1.93 (2.71)	2.16 (3.02)	2.36 (3.30)	$1.1^{2.1}_{0.5}$	$1.5^{3.0}_{0.8}$
BRI0952 − 0115	6.6	2.09 (2.58)	2.70 (3.33)	3.28 (4.04)	3.74 (4.61)	$3.5^{4.0}_{2.7}$	$4.4^{5.2}_{3.5}$
Q1017 − 207	6.8	2.63 (6.33)	3.36 (8.09)	4.02 (9.67)	4.60 (11.06)	$4.3^{13.0}_{1.4}$	$6.4^{19.0}_{2.3}$
HE1104 − 1805	6.6	48.1 (63.47)	62.1 (81.90)	75.3 (99.37)	85.9 (113.41)	$22.8^{51.2}_{12.7}$	$36.6^{63.7}_{23.1}$
LBQ1009 − 025	6.7	8.02 (11.23)	10.1 (14.15)	11.8 (16.53)	13.5 (18.92)	$5.5^{7.9}_{4.2}$	$7.4^{9.8}_{5.0}$
B1030 + 071	9.4	10.5 (17.88)	12.9 (22.27)	14.7 (25.06)	16.5 (28.09)	$10.6^{15.3}_{6.5}$	$14.5^{21.3}_{8.3}$
SBS1520 + 530	7.6	12.6 (17.64)	16.0 (22.41)	18.8 (26.38)	21.2 (29.67)	$18.5^{30.9}_{11.2}$	$21.8^{34.1}_{11.9}$
HE2149 − 274	7.1	7.34 (14.17)	9.31 (17.98)	11.0 (21.30)	12.5 (24.24)	$4.6^{6.7}_{3.6}$	$6.9^{8.9}_{5.0}$

Table II (column 2) also shows the ratio ($\langle\nabla\Phi_N\rangle/\mathfrak{a}_0$) of the geometric mean of the Newtonian gravity at the closest approaches to Milgrom's constant, $\mathfrak{a}_0$. The ratio indicates what regimes the lensing systems belong to. As shown in the last paragraph of Sec. II E, this ratio depends on the mass enclosed within the radii of the closest approach, so it varies with the choice of $\tilde{\mu}$. However, since the choice of $\tilde{\mu}$ only influences the total masses in our 10 systems up to 50%, different choices of $\tilde{\mu}$ will not affect our conclusion about to which regime are these systems belong to. Here, we choose the masses inferred from GR (that is, $\tilde{\mu} = 1$) to calculate $\langle\nabla\Phi_N\rangle/\mathfrak{a}_0$ in the second column of Table II. According to the values of this criterion, all 10 systems are in the intermediate MOND regime (that is, $\langle\nabla\Phi_N\rangle$ neither $\gg \mathfrak{a}_0$ nor $\ll \mathfrak{a}_0$). We should remind that our indicator, $\langle\nabla\Phi_N\rangle/\mathfrak{a}_0$, is slightly different from the conventional $\nabla\Phi/\mathfrak{a}_0$ because in a double-image system, two different light rays could likely penetrate through two different regimes. Take FBQ0951 + 2635 for example, where we have the highest value of $\langle\nabla\Phi_N\rangle/\mathfrak{a}_0$, although one light ray definitely passes through the Newtonian regime, the other penetrates a regime with $\nabla\Phi_N/\mathfrak{a}_0 \sim 3$, in which $\nabla\Phi$ is 5% higher than $\nabla\Phi_N$ for the standard form, 24% for the simple form, and 54% for Bekenstein's form. This is consistent with the finding that the choice of $\tilde{\mu}$ has a significant influence on the inferred lensing masses.

Figure 4 shows the mass ratio of TeVeS to GR for the 10 lensing systems. For comparison of mass differences between the three forms, all ratios are plotted against $\langle\boldsymbol{\nabla}\Phi_N\rangle/\mathfrak{a}_0$. We find that the ratio increases slightly with $\langle\boldsymbol{\nabla}\Phi_N\rangle/\mathfrak{a}_0$. This does make sense because a smaller $\langle\boldsymbol{\nabla}\Phi_N\rangle/\mathfrak{a}_0$ means that the system is closer to the MOND regime, and a larger mass discrepancy is expected. Figure 4 also shows the comparison between our results of lensing mass and stellar mass given by Ferreras *et al.* [28].

Table III lists our estimates of lensing mass for the standard ΛCDM cosmology ($\Omega_m = 0.3$, $\Omega_\Lambda = 0.7$, $h = 0.7$). It appears that in TeVeS, the difference of lensing mass between the standard ΛCDM cosmology and νHDM cosmology is less than 2%. This result also indicates that our results will essentially hold also for the single-sterile neutrino cosmology with $\Omega_b, \Omega_\nu, Omega_\Lambda, h = 0.05, 0.24, 0.7, 0.7$ in [15].For comparison, we also list the lensing mass estimated by Ferreras *et al.* [27] in the columns 5 & 7 of Table III. Although our total lensing masses are compatible with their total lensing mass under the formalism of GR, we have systematically smaller values than theirs in the case of TeVeS. This is consistent with our expectation because as shown in Fig. 2, for an identical choice of the form of $\tilde{\mu}$, the formalism of Eq. (1) always leads to stronger gravity, so less mass, than that of Eq. (27).

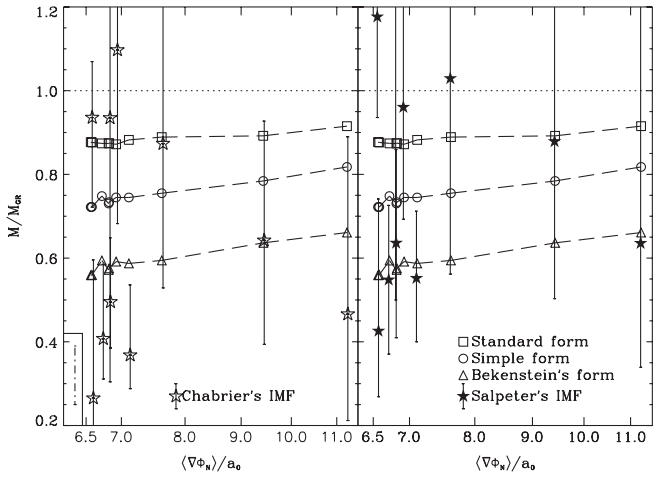

FIG. 4. Mass ratio of MONDian to GR lensing mass. We also include the ratio of the stellar mass estimated from stellar histories with Chabrier's (left panel) and Salpeter's (right panel) IMFs to the GR lensing mass ($M_{\rm GR}$). All lensing masses are calculated based on a Hernquist model. The typical uncertainty of the lensing mass is shown at the left-bottom corner. It appears that there is a huge mass discrepancy between conventional gravity and TeVeS.

TABLE III. Lensing mass estimates for three particular forms of $\tilde{\mu}(x)$ in the standard ΛCDM cosmology. The total mass of the lens in unit $10^{10}M_{\odot}$ is listed in columns 2–4. The uncertainty of masses can be up to 10% because of the uncertainty of effective radius. For comparison, the MONDian and GR lensing masses in [17] are also cited.

	M_L(TeVeS)/$10^{10}M_{\odot}$			M_L(GR)/$10^{10}M_{\odot}$		
Lens	Bekenstein	Simple	Standard	FSY08[a]		FSY08
Q0142 − 100	19.39	24.32	28.34	29.28	32.29	32.37
HS0818 + 1227	29.59	37.64	44.68	46.31	50.80	50.99
FBQ0951 + 2635	2.20	2.72	3.04	3.82	3.30	4.07
BRI0952 − 0115	2.59	3.35	4.05	6.62	4.60	7.33
Q1017 − 207	6.41	8.17	9.69	9.04	10.95	9.93
HE1104 − 1805	64.53	82.99	99.76	103.17	112.67	112.93
LBQ1009 − 025	11.65	14.65	17.02		19.28	
B1030 + 071	18.09	22.27	25.22		28.00	
SBS1520 + 530	17.92	22.68	26.51		29.57	
HE2149 − 274	14.33	18.14	21.36		24.14	

[a]Ferreras *et al.* (2008).

Figure 5 compares the mass difference between the lensing mass and the stellar mass. Although there is a significant scattering in the data due to the large uncertainty of stellar masses, the average over the 10 systems shows no obvious requirement of dark matter for Bekenstein's and the simple form while compared with stellar mass estimated from Chabrier's IMF. On the other hand, the lensing masses inferred from the simple form and the standard form are almost identical to the stellar masses estimated from Saltpeter's IMF. We also plot the same comparison for the MONDian lensing mass in Ferreras *et al.* [17] and for the lensing mass estimated in the standard cosmology by Ferreras *et al.* [28]. It turns out that the average mass difference ($\triangle M/M$) for the MONDian lensing masses in Ferreras *et al.* [17] (dashed line in Fig. 5) is even higher than its counterpart for the GR lensing masses in Ferreras *et al.* [28] (dashed-triple dotted line in Fig. 5), not to mention our estimates of MONDian mass. This might be because that Ferreras *et al.* (2008) [17] have wrongly compared the total the MONDian lensing mass with the aperture stellar mass.

IV. DISCUSSION

In our analysis, the simple form of $\tilde{\mu}(x)$ (i.e., $\alpha = 1$, $\eta = 1$ in the canonical form (24)) yields, on average, a lensing mass compatible with the stellar mass estimated from population synthesis models with Salpeter's and Chabrier's IMF. The mass differences between the lensing mass and stellar mass are around 10%, which is compatible

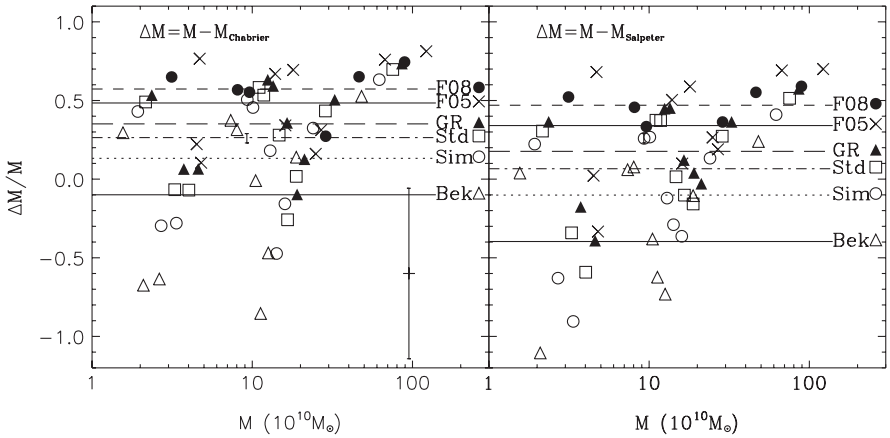

FIG. 5. Contribution of dark matter to the mass budget from a comparison between MONDian lensing mass and stellar mass given by [28]. We also include MOND-like lensing mass in [17] and GR lensing mass [28]. M is the lensing mass from different models. The averages of the mass differences are plotted for Bekenstein's form (solid line), the simple form (dotted line), the standard form (dotted-dashed line), GR (long dashed line), MONDian lensing in FSY08 (dashed line), and GR lensing mass in FSW05 (dashed-triple dotted line). It appears that [27] has compared MONDian total lensing mass with aperture stellar mass, so leads to the higher requirement for dark matter budget. The typical uncertainty of stellar mass is shown at the right corner of the left panel.

to the uncertainty in the lensing mass. The simple form also yields an average of 25% mass discrepancy between the inferred lensing mass of TeVeS and GR. This is close to the 30% value estimated by Sanders [46]. On the other hand, Bekenstein's form gives an average of 41%, and provides a better fit to lower-mass IMFs ($M_{\rm Chab}$). This is consistent with the conclusion of Romanowsky *et al.* [47], where a preference of Bekenstein's form is drawn from star formation histories based on lower-mass IMFs.

Our analysis also shows that when we use $M_{\rm Chab}$ as the mass of lens, the standard form has a problem in producing enough angle of deflection in strong lensing. This coincides with the conclusion of studies on the dynamics of spiral galaxies [9,32,33]. It is quite reasonable because both gravitational lensing and the dynamics of spiral galaxies comes from the change of gravity (see Possion Eq. (1)).

Because of the significant uncertainty in stellar mass given by [28], it is premature to claim which choice of the interpolation function $\tilde{\mu}(x)$ in the MONDian paradigm is favored by elliptical galaxy lensing observations. However, our study shows that, like spiral galaxies, elliptical galaxies can be used to distinguish different forms of $\tilde{\mu}(x)$ as well. We believe that with an independently precise measurement of mass of elliptical galaxies, strong gravitational lensing can offer us a window to study the form of $\tilde{\mu}(x)$. We will explicitly write down a formalism for this application in the future.

We should point out that our analysis is based heavily on the assumption that the lenses in these systems are spherical and quasistatic in order to use Eq. (4) to derive the lensing equation. However, the assumption of spherical distribution is not always sufficient for most known lenses. Moreover, the choice of mass model for the lens may also affect the inference of the total mass of the lens. Thus, it is worthwhile to study how the deviation from this assumption would affect our conclusion here. We note that while a spherical Hernquist model is a reasonable assumption for most lenses here, it is always a poor assumption for modeling rotation curves of spiral galaxies which often have exponential disk profiles, and the gravity is enhanced in the disk plane. In this regard, the recent claim of inconsistency of lensing and galaxy rotation curve in MOND [27] has yet to be corrected for these systematic effects. For systems in a cluster environment, which are not yet in full dynamical equilibrium, it might be important to include nontrivial effects of the vector field [48,49].

In Ferreras *et al.* [17], they concluded that MOND might have problems in explaining galactic lensing systems, i.e. dark matter is still needed. Our analysis differs from their conclusion. Perhaps the reason is that they have not only applied the formalism of Eq. (27) in their calculation, but have also drawn their conclusion by comparing total lensing mass with aperture stellar mass. Indeed, the first reason might also explain why Mavromatos *et al.* [26] have found a considerable discrepancy between MOND and TeVeS (they unconventionally refer to *MOND* as solving for lensing mass by Eq. (27) and refer to *TeVeS* as solving the full relativistic equations from first principles). Mavromatos *et al.* [26] have discussed lensing mass in TeVeS for three specific forms of $\tilde{\mu}$ that are corresponding to $(\alpha, \eta) = (1, -1)$, (1, 0) and (1, 1) for the canonical interpolation function, Eq. (24). We do not discuss the case of $(\alpha, \eta) = (1, -1)$ (or $\alpha = -1$ in [26]) because it fails to lead to the Newtonian limit (see Fig. 1). The other two choices of the interpolation function in [26] are identical to Bekenstein's and the simple form in this paper, respectively. Thus, it is not surprising that their estimates of lensing mass are compatible with ours because the geodesic equations, Eqs. (6)–(8), in our calculations are also derived from first principles with a simple assumption of spherical symmetry. However, Mavromatos *et al.* [26] have drawn a conclusion completely opposite to ours. We attribute this contradictory result to sample bias. Somehow, 5 out of the 6 lensing systems they chose have $\Delta M > 0$, but when we consider all 10 available lensing systems, the bias is gone (compare Fig. 5 of this paper to Fig. 2 of [26]). Moreover, we stress that uncertainty should play a role in discussion. While considering the significant uncertainty of stellar mass and the potential error of estimates of lensing mass, while mild deviations exist, we found no strong cases of outliers to the TeVeS model.

We conclude that our procedure to estimate lensing mass is consistent with the method of Mavromatos *et al.* [26], where modified Einstein equations are fully solved, but our studies on the 10 systems do not show any apparent need for *ad hoc* dark matter in elliptical galaxies. This, of course, does not mean GR fails to explain the observation if certain dark matter model is assumed. Moreover, statistically TeVeS seems to fit these systems reasonably well with a simple, spherically symmetric lens model. This differs from the conclusion of Ferreras *et al.* [17], but sides with Zhao *et al.* [18] and Shan *et al.* [19], where a constant mass-to-light ratio is assumed. However, due to the significant uncertainty of stellar masses given by [28], our conclusion is meaningful only at the statistical, but not the individual level. A more accurate and independent estimation of the mass of the lenses is still required in order to compare the lensing masses obtained here for a higher precision. One potential possibility is to estimate the mass of elliptical galaxies from velocities of dispersion and then compare them with lensing mass under a consistent framework [25].

ACKNOWLEDGMENTS

We thank Jacob Bekenstein, Martin Feix, and Keith Horne for their helpful comments, and thank Jeremy Barber for his help in English editing. M. C. C. is partly

supported by SUPA(UK), and would like to thank Andy Taylor for helpful discussion. C. M. K. and Y. T. are supported, in part, by the Taiwan National Science Council Grant Nos. NSC 98-2923-M-008-01-MY3 and NSC 99-2112-M-008-015-MY3. H. Z. acknowledges numerous hospitalities at University of Edinburgh and thanks especially Andy Taylor for discussions. C. M. K. is grateful to S. Kwok and K. S. Cheng for their hospitality during his leave at Department of Physics, College of Science of University of Hong Kong.

[1] M. Tegmark *et al.*, Phys. Rev. D **74**, 123507 (2006).
[2] J. D. Bekenstein, Phys. Rev. D **70**, 083509 (2004).
[3] M. Milgrom, Astrophys. J. **270**, 365 (1983).
[4] M. Milgrom, Phys. Rev. D **80**, 123536 (2009).
[5] H. S. Zhao and B. Li, Astrophys. J. **712**, 130 (2010).
[6] S. Dodelson and M. Liguori, Phys. Rev. Lett. **97**, 231301 (2006).
[7] C. Skordis, D. F. Mota, P. G. Ferreira, and C. Boehm, Phys. Rev. Lett. **96**, 011301 (2006).
[8] R. H. Sanders and S. S. McGaugh, Annu. Rev. Astron. Astrophys. **40**, 263 (2002).
[9] B. Famaey, G. Gentile, J.-P. Bruneton, and H. S. Zhao, Phys. Rev. D **75**, 063002 (2007).
[10] D. Clowe, A. Gonzalez, and M. Markevitch, Astrophys. J. **648**, L109 (2006).
[11] G. W. Angus, H. Y. Shan, H. S. Zhao, and B. Famaey, Astrophys. J. **654**, L13 (2007).
[12] G. W. Angus, Mon. Not. R. Astron. Soc. **394**, 527 (2009).
[13] G. W. Angus, B. Faymaey, and A. Diaferio, Mon. Not. R. Astron. Soc. **402**, 395 (2010).
[14] P. Natarajan and H. S. Zhao, Mon. Not. R. Astron. Soc., **389**, 250 (2008).
[15] M. Feix, H. S. Zhao, C. Fedeli, J. L. G. Pestana, and H. Hoekstra, Phys. Rev. D **82**, 124003 (2010).
[16] S. Tremaine and J. E. Gunn, Phys. Rev. Lett. **42**, 407 (1979).
[17] I. Ferreras, M. Sakellariadou, and M. F. Yusaf, Phys. Rev. Lett. **100**, 031302 (2008).
[18] H. S. Zhao, D. J. Bacon, A. N. Taylor, and K. Horne, Mon. Not. R. Astron. Soc. **368**, 171 (2006).
[19] H. S. Shan, M. Feix, B. Famaey, and H. S. Zhao, Mon. Not. R. Astron. Soc. **387**, 1303 (2008).
[20] B. Qin, X. P. Wu, and Z. L. Zou, A&A International **296**, 264 (1995).
[21] D. J. Mortlock and E. L. Turner, Mon. Not. R. Astron. Soc. **327**, 557 (2001).
[22] M. C. Chiu, C. M. Ko, and Y. Tian, Astrophys. J. **636**, 565 (2006).
[23] M. Feix, C. Fedeli, and M. Bartelmann, A&A International **480**, 313 (2008).
[24] M. Feix, D. Xu, H. Y. Shan, B. Famaey, M. Limousin, H. S. Zhao, and A. Taylor, Astrophys. J. **682**, 711 (2008).
[25] M. C. Chiu, Y. Tian, and C. M. Ko, in *Proceedings of the 10th Asian-Pacific Regional IAU Meeting 2008* (World Scientific, London, 2007).
[26] N. E. Mavromatos, M. Sakellariadou, and M. F. Yusaf, Phys. Rev. D **79**, 081301 (2009).
[27] I. Ferreras, N. E. Mavromatos, M. Sakellariadou, and M. F. Yusaf, Phys. Rev. D **80**, 103506 (2009).
[28] I. Ferreras, P. Saha, and L. Williams, Astrophys. J. **623**, L5 (2005).
[29] E. Sagi, Phys. Rev. D **80**, 044032 (2009).
[30] C. Skordis, Phys. Rev. D **77**, 123502 (2008).
[31] C. R. Contaldi, T. Wiseman, and B. Withers, Phys. Rev. D **78**, 044034 (2008).
[32] B. Famaey and J. Binney, Mon. Not. R. Astron. Soc. **363**, 603 (2005).
[33] H. S. Zhao and B. Famaey, Astrophys. J. **638**, L9 (2006).
[34] H. S. Zhao and B. Famaey, Phys. Rev. D **81**, 087304 (2010).
[35] S. S. McGaugh, Astrophys. J. **523**, L99 (1999).
[36] S. S. McGaugh, Astrophys. J. **611**, 26 (2004).
[37] S. Dodelson, E. Gates, and A. Stebbins, Astrophys. J. **467**, 10 (1996).
[38] N. A. Bahcall, J. P. Ostriker, S. Perlmutter, and P. J. Steinhardt, Science **284**, 1481 (1999).
[39] S. Hanany *et al.*, Astrophys. J. **545**, L5 (2000).
[40] G. de Vaucouleurs, Ann. d'Ap. **11**, 247 (1948).
[41] L. Hernquist, Astrophys. J. **356**, 359 (1990).
[42] D. Rusin *et al.*, Astrophys. J. **587**, 143 (2003).
[43] http://www.cfa.harvard.edu/castles/.
[44] G. Chabrier, Publ. Astron. Soc. Pac. **115**, 763 (2003).
[45] E. E. Salpeter, Astrophys. J. **121**, 161 (1955).
[46] R. H. Sanders, Mon. Not. R. Astron. Soc. **389**, 701 (2008).
[47] A. J. Romanowsky *et al.* (unpublished).
[48] I. Ferreira and G. Starkman, Science **326**, 812 (2009).
[49] H. S. Zhao, Astrophys. J. **671**, L1 (2007).